厚生労働科学研究費補助金
ヒトゲノム・再生医療等研究事業

脊髄小脳変性症の新規遺伝子の同定と治療法の開発

14年度　総括・分担研究報告書

主任研究者：水 澤 英 洋

平成15（2003）年4月

目　次

厚生科学研究費補助金（ヒトゲノム・再生医療等研究事業）
総括研究報告書

脊髄小脳変性症の新規遺伝子の同定と治療法の開発

主任研究者　水澤英洋　東京医科歯科大学医歯学総合研究科脳神経機能病態学教授

研究要旨　　我々は本邦に存在する原因不明の遺伝性脊髄小脳変性症の中では最も頻度が高いと考えられる第 16 番染色体長腕に連鎖する常染色体優性遺伝性皮質性小脳萎縮症(16q-linked ADCCA)の原因遺伝子を同定する研究を行ってきた。16q-linked ADCCA 遺伝子が存在する 5 メガベース(Mb)程の領域を昨年度完全な contig にした。本年度は患者家系を 30 家系に増やし、候補領域内のマーカーによるハプロタイプ解析から、候補領域を 1Mb 以下の領域に縮小することができた。さらにこの領域に存在する遺伝子群について変異のスクリーニングを行った。現在までのところ原因遺伝子の同定には至っていないが、患者に共通して認められ、一般健常人には認められない variation を見いだしており、変異同定は近い将来可能と期待している。

分担研究者　石川欽也　東京医科歯科大学医学部附属病院助手
横田隆徳　東京医科歯科大学医学部附属病院講師

A.　研究目的

本研究の目的は、本邦に存在する原因不明の遺伝性脊髄小脳変性症のうち最も頻度が高いと思われる病型、すなわち第 16 番染色体長腕に連鎖する常染色体優性遺伝性皮質性小脳萎縮症(16q-linked ADCCA)の原因遺伝子を同定することである。具体的には昨年度遺伝子変異が存在する候補領域を限定化したことに基づいて、ポジショナル・クローニング(positional cloning)の最終的な段階である遺伝子変異の検索を進める。すなわちその候補領域内に存在する遺伝子について逐次患者での変異の有無を解析し、遺伝子変異を同定したいと期待している。遺伝子変異が同定されれば、この遺伝子の本来の機能を明らかにし、遺伝子変異がどのように疾患の発症をもたらすかを解明することにより、それらの情報に基づき新しい治療法の開発が可能となる。

本研究の必要性は、本病型が現在のところ原因不明でかつ有効な治療法がない神経難病であることからも明らかであるが、さらにこの病型の頻度が我々の統計では全優性遺伝性失調症の約 15%程度を占める、高いものであることからも明らかである。なお、本病型は同様な症候を呈する脊髄小脳失調症 6 型(SCA6)を含め脊髄小脳変性症の中で最も高齢で発症することが特徴である。

原因遺伝子が同定できれば、本疾患の正確な病態の解明と、ひいては発症機序に基づいた治療法の確立に大きく寄与すると期待される。本疾患に類似した臨床像を呈する失調症の家系がアメリカやドイツ、イギリス、オーストラリアなど海外の広い地域からも記載されていることや、同じ領域に連鎖するものの、臨床症状の大きく異なる家系が脊髄小脳失調症 4 型(SCA4)としてアメリカやドイツから報告されていることから、本研究により原因遺伝子が解明されれば、世界的にもこの領域の研究の推進に大きく貢献するものと期待される。

B.　研究方法

候補領域を限定化することにより、より早く変異の同定に至ることができる。このため、今年度は北海道から九州に至るほぼ全国に分布する 11 施設より類似する患者家系の DNA を供与していただいた。その患者 DNA について昨年度までに報告した共通ハプロタイプ(Takashima et al. J Hum Genet, 2001)の有無を解析した。また、本施設における類似症例についても同様に検索し、全症例で共通する最大のハプロタイプ領域を新たな候補領域と定めることにした。

遺伝子変異のスクリーニングについては、まずその基礎になる物理地図を、昨年までに３３個の BAC クローンの連続からなる約 5Mb 長の contig として完成させた(Li. M et al. J Hum Genet 2003)。次にこの染色体領域の DNA 塩基配列情報を NCBI (National Center for Biotechnology Information) (http://www.ncbi.nlm.nih.gov/entrez/) や Ensembl (http://www.ensembl.org/) などから取得した。最終的な変異の同定のための戦略には脳に発現する遺伝子内の点変異などの静的変異(static mutation)を想定した探索と、これまでの優性遺伝性失調症に共通して見られる３塩基(CAG)などの繰り返し配列が異常伸長する動的変異(dynamic mutation)を想定した探索の２種類を行う必要がある。このため、以下の方法によって遺伝子変異を検索することにした。

静的変異の探索：候補領域に存在することが報告されている全ての遺伝子について、まず DNA レベルでの塩基配列情報を特にエクソン(exon)とイントロン(intron)の境に留意して収集。また、各遺伝子が脳などの組織でどのように転写され発現しているか、といった RNA(メッセンジャーRNA: mRNA)レベルでの発現情報も集積した。

次にこれを元に各遺伝子について全ての判明し得た exon 領域についてその近傍の intron を含めて PCR で増幅するために primer を設定。各 exon について PCR で患者および健常者の DNA をそれぞれ増幅し、PCR 産物の塩基配列を直接蛍光自動シークエンサー(ABI PRISM™ 377 Sequencer)で解析した。実験によって得られた塩基配列をデータベースと照合し、点変異などの変異の有無を解析した。この領域に存在する遺伝子について、その機能によりあらかじめ本疾患の候補遺伝子と想定し解析を優先させること、すなわち positional-candidate approach をとることは困難であった。このため全ての遺伝子をスクリーニングすることにした。これまでに解析した遺伝子は 30 を越えた。

動的変異の検索：昨年度までにすでに CAG を含む３塩基配列はもちろん、２塩基配列、４塩基配列、５塩基配列などの反復配列(リピート)について、患者に特異的な異常伸長変異の有無を検索してきたが、今回の候補領域については、繰り返し回数の少ない反復配列についても、異常伸長の可能性を考えて解析した。この反復配列の同定には、ソフトウエアーRepeatMasker (http://ftp.genome.washington.edu/cgi-bin/RepeatMasker) や Tandem Repeat Finder (http://c3.biomath.mssm.edu/trf.html) を用い、塩基配列が解読され公表された BAC クローンについて NCBI データベースからダウンロードし、ソフトウエアー上で解析する。この方法によって、繰り返し配列の途中に interruption sequence が挿入されたような複雑な反復配列でも検出が可能である。また、最小リピートとしては 3 回繰り返しのものでも同定可能である。これまでの繰り返し配列の異常伸長を考慮すると、健常者では最低でも 11 回～13 回の繰り返し配列であることから、この検索でほぼ充分スクリーニングできると想定できる。

この方法によって同定した反復配列について、昨年度と同様に逐次健常日本人での遺伝的多型性(heterozygocity)を解析する。次に全てのマーカーについて患者家系でのハプロタイプ解析を行う。いずれの場合も反復配列を挟むように蛍光標識したプライマーをデザインし、PCR 法にて DNA を増幅後、ALF™ Automated DNA Sequencer II (Amersham Pharmacia Biotech)で遺伝子型(genotype)を決定する。さらに全家系でハプロタイプが共通する領域が有るかを検索し、その領域を新たに限定された候補領域と定めた。同時に全国から類似の家系・症例を同意の元に照会していただき、共通するハプロタイプを有する家系を検索し、昨年度までより家系を増やして候補領域をできる限り狭める努力も継続して行う。

関連疾患、脊髄小脳失調症 6 型(SCA6)の病態解明のための研究:SCA6 は先述の通り 16q-linked ADCCA と臨床的に類似点が多く、かつ本邦では最も頻度の高い優性遺伝性失調症の一つである。我々はこの疾患の連鎖解析により世界で初めて遺伝子座を同定している。SCA6 はヒトα1A-カルシウムチャネル遺伝子内の CAG 繰り返し配列が異常に伸長するために発症する。我々は SCA6 の病態解明のため、患者脳での変異蛋白の発現と神経細胞死の関連について研究した。また培養細胞を用いて細胞死の機序を研究した。これらの研究成果は 16q-linked ADCCA の原因解明およびその後の治療法開発のためにも重要であると言える。

倫理面での配慮：倫理面への配慮については、平成 12 年 4 月の厚生科学審議会の指針にもとづき本施設において新設された遺伝子研究のための倫理審査委員会の審議を経て許可されており、動物の取り扱いも本学動物実験委員会の指針に基づいて行うなど十分な配慮がなされている。

C. 研究結果

1) 候補領域の限定化：これまでに合計 30 を越す家系および家族歴を有する患者を集積し、昨年度報告した共通ハプロタイプの有無を検索したところ、1Mb 領域以下に相当する領域にのみハプロタイプが共通することが分かった。逆にその他の領域ではハプロタイプが少数の家系では異なっていた。この共通するハプロタイプは健常者では認められず、このハプロタイプの同定により、かなり高い確率で遺伝子診断が可能であると考えられる。現在健常者の家系を用いての健常者ハプロタイプを解析し、この中では患者に共通するハプロタイプが存在する確率が低いことを証明するべく検索をしている。

2) 静的遺伝子変異の検索：今年度多数の遺伝子で点変異を含む遺伝子変異のスクリーニングを行った。研究の性質上、その詳細は報告できないが、遺伝子が密に存在する染色体領域が含まれており、その中から遺伝子変異を発見することは容易ではなかった。現在までのところ、明らかな変異の同定には至っていない。しかし、この過程で患者にのみ共通し、一般健常者には全く認められない遺伝子多型を呈するマーカー

を２つ見いだした。すなわち 16q-linked ADCCA の原因遺伝子は本候補領域内に存在することは間違いないと考えられる。現在、可能な限り登録されている残りの遺伝子のスクリーニングを行うと共に、未公表の遺伝子についても解析を進めている。

3) 動的遺伝子変異の検索：新たな解析ソフトウエアーも用いて、候補領域内の小さな反復配列を含むマーカーを検索し、合計 99 個の反復配列を同定した。この内の 63 個について患者と健常者 DNA での繰り返し回数の違いを検討した。その結果患者に特異的な異常伸長は認められず、現在のところ本疾患の発症機序に繰り返し配列の異常伸長が関連している可能性は肯定できない。一方、検索した範囲で新たに多型性 DNA マーカーを 7 個同定し、これらのマーカーでのハプロタイプを加えることにより、候補領域を限定化することができた。

4) SCA6 脳における変異蛋白の発現と培養細胞での細胞死の研究：まず患者脳を用いた免疫組織化学により、最も変性する Purkinje 細胞の細胞質を中心に変異カルシウムチャネル蛋白と異常伸長ポリグルタミン鎖を有する蛋白の２種類が凝集していることが判明した。ウエスタンブロットでは、カルシウムチャネル蛋白の発現は低下しておらず、異常伸長ポリグルタミンの発現は少なくとも変異蛋白の発現に影響していないことが分かった。一方、培養細胞に全長の変異チャネル遺伝子を導入すると、正常遺伝子を導入した場合より有意に細胞死が強く誘導されることが判明し、変異遺伝子が細胞毒性を有することが証明された。またポリグルタミン鎖を含むカルシウムチャネル蛋白の C 末端側蛋白が断片化されて細胞内で凝集していることが示唆された。さらにこの部分蛋白を細胞に強制発現させると更に強い細胞死が誘導され、SCA6 においてカルシウムチャネル蛋白の断片化が細胞死に関与している可能性が初めて示された (Kobodera T. et al., 2003)。

D. 考察

昨年度、我々の有する患者家系では、たとえ日本国内の異なる地域を出身地としても発症者ではある区間の染色体領域については共通するハプロタイプを有していること、すなわち創始者効果が存在すること、を明らかにした。実は本疾患の様に創始者効果を有する疾患のポジショナル・クローニングでは候補領域を限定化することが難しい場合がある。多数の家系を解析し、ハプロタイプの異なる家系に遭遇する必要があるが、本疾患のように高齢発症が特徴である場合、家系の集積自体が困難であるからである。このようなことから今年度我々は、北海道から九州地方に及ぶ広い範囲の施設の協力を得て多数の家系・患者を集積した。これほど多い家系の集積は世界的にも例がない。後に記載する候補領域内の新たな多型性 DNA マーカーの同定とも併せて、多数の家系でのハプロタイプを決定した結果、候補領域を 1Mb 程度の狭い領域に限定化することができた。この領域の外では患者間で異なるアレル(allele)を持つ例が存在し、家系間でハプロタイプが共通しなくなる。また、連鎖不平衡解析でもこの領域の外側では不平衡関係が崩れる。したがって、ハプロタイプが共通する狭い領域が新たな候補領域であると考えられ、この領域内に原因となる遺伝子の変異が存在する可能性が高い。

この候補領域内には、ヒト染色体での通常あるいは平均的な遺伝子密度を遙かに越えて、多くの遺伝子が存在する部位が含まれていた。このため、候補領域の限定化の他にも遺伝子同定上、困難な条件が加わっている。我々は今年度この領域内の遺伝子群についてかなり綿密な変異スクリーニングを行い、30 以上の遺伝子について患者での変異の有無を検索し終えた。この範囲では変異はなく、残るわずかの領域に遺伝子変異があるか、点変異以外の変異パターンの解析を行う必要があると考えている。

我々はこの候補領域内で、独自に２種類のソフトウエアーを用いて新たな多型性マーカーを７個発見した。これらについて新たな家系を含めて解析し、候補領域を絞り込むことに成功した。このうち、患者に共通して認められ、健常者には全く存在しないアレルを示す極めて連鎖不平衡の高いマーカーを見いだした。これにより、理論的には 16q-ADCCA の遺伝子診断が可能になった。さらにこのマーカーを用いた診断では、本疾患の遺伝子頻度は我々の有する全優性遺伝性失調症の中の 17%と高いことが判明した。この結果には集積の段階で bias が関与していることも考える必要があるが、16q-linked ADCCA の頻度はこれまで知られていたより高い可能性を示唆していると言える。

これまでの優性遺伝性失調症の原因はいずれも繰り返し配列の異常伸長であることから、これまで我々は繰り返し配列の異常伸長の有無を患者 DNA で解析してきた。しかし検索した範囲内では異常伸長は認められなかった。残された繰り返し配列に異常伸長がある可能性は否定できないが、これら残りの反復配列は繰り返し回数が少ないものがほとんどで、多型性すら示す可能性が低く、本疾患の原因となる可能性は非常に低いと考えられた。すなわち、本疾患の原因となる変異には繰り返し配列の異常伸長以外の新しい変異パターンが関与している可能性がますます高くなり、ユニークな発症機序を秘め

ている可能性が挙げられた。

E. 結論

本年度日本中の地域から患者家系を集積し候補領域を確実に限定化し、その領域内の綿密な遺伝子変異のスクリーニングを直接シークエンスと、PCR による繰り返し配列の異常伸長の有無の解析の両面から行った。16q-linked ADCCA の原因遺伝子は未だ同定できていないが、確実に候補を絞り込んでおり、近い将来同定が可能と予測している。本疾患の原因には繰り返し配列の異常伸長以外のユニークな機序が関連している可能性が挙げられた。

F. 研究発表

1. 論文発表

1) Tsunemi T, Saegusa H, Ishikawa K, Nagayama S, Murakoshi T, Mizusawa H, T. Tanabe: Novel Cav2.1 splice variants isolated from purkinje cells do not generate P-type Ca2+ current. J Biological Chemistry 277(9): 7214-7221, 2002.
2) Ohara S, Iwahashi T, Oide T, Hayashi R, Nakajima T, Ishikawa K, Mizusawa H: Spinocerebellar ataxia type 6 with motor neuron loss: A follow-up autopsy report. J Neurol 294: 633-635, 2002.
3) Miake H, Mizusawa H, Iwatsubo T, Hasegawa M: Biochemical characterization of the core structure of α-synuclein filaments. J Biological Chemistry 277(21): 19213-19219, 2002.
4) Kubodera T, Yokota T, Ohwada K, Ishikawa K, Miura H, Matsuoka T, Mizusawa H: Proteolytic cleavage and cellular toxicity of the human α 1A calcium channel in spinocerebellar ataxia type 6 (SCA6). Neuroscience Letters 341:74-78, 2003.
5) Li M, Ishikawa K, Toru S, Tomimitsu H, Takashima M, Goto J, Takiyama Y, Sasaki H, Imoto I, Inazawa J, Toda T, kanazawa I, Mizusawa H. Physicqal map and haplotype analysis of 16q-linked autosomal dominant cerebellar ataxia (ADCA) type III in Japan. J Hum Genet 48:111-118, 2003.
6) Mizusawa H: Spinocerebellar ataxia type 4 (SCA4). (Stefan M. Pulst), Genetics of movement disorders, Academic press, 71-73, 2002.
7) 常深泰司, 水澤英洋: ポリグルタミン病ー脊髄小脳失調症6型を中心に一. 医学のあゆみ 201: 1133-1142, 2002.
8) 水澤英洋: 核内封入体を伴わないポリグルタミン病. 神経研究の進歩 46: 637-645, 2002.
9) 水澤英洋: Triplet repeat 病研究の進歩. 組織培養工学 28: 50-51, 2002.
10) 融 衆太, 水澤英洋: 核封入体を作らない CAG リピート病 -脊髄小脳失調症 6 型-. 組織培工学 28:11-14, 2002.

2. 学会発表

1) Ishikawa K, Ishida K, Fujigasaki H, Owada K, Mizusawa H: The expression of polyglutamine and α 1A-voltage-dependent calcium channel protein in the SCA6 brain. The 52th Annual Meetings, the American Society of Human Genetics, (Baltimore), 2002.10.15-19.
2) 融 衆太、石川欽也、李 明順、後藤 順、金澤一郎、瀧山嘉久、佐々木秀直、三谷和子、水澤英洋 第 16 番染色体長腕に連鎖する優性遺伝性皮質性小脳萎縮症の臨床的検討 第 43 回日本神経学会総会, (札幌), 2002. 5. 29-31
3) 石川欽也、藤ヶ崎浩人、石田和之、大越教夫、加藤丈夫、庄司進一、水澤英洋:SCA6 脳内のα1A-Ca チャネル蛋白発現量. 第 43 回日本神経学会総会, (札幌), 2002. 5. 29-31
4) 李 明順、融 衆太、冨満弘之、石川欽也、水澤英洋:第 16 番染色体に連鎖する常染色体優性遺伝性皮質性小脳萎縮症の候補遺伝子の検討. 第 43 回日本神経学会総会, (札幌), 2002. 5. 29-31

G. 知的所有権の取得状況

とくになし

H. 健康危険情報

とくになし

別紙５

研究成果の刊行に関する一覧表

書籍

著者氏名	論文タイトル名	書籍全体の編集者名	書 籍 名	出版社名	出版地	出版年	ページ
Mizusawa H	Spinocerebellar ataxia type 4 (SCA4).	Stefan M.	Academic press	Genetics of movement disorders	San Diego	2002	71-73

雑誌

発表者氏名	論文タイトル名	発表誌名	巻号	ページ	出版年
Tsunemi T, Saegusa H, Ishikawa K, Nagayama S, Murakoshi T, Mizusawa H, T. Tanabe	Novel Cav2.1 splice variants isolated from Purkinje cells do not generate P-type Ca2+ current.	J Biological Chemistry	277	7214-7221	2002
Ohara S, Iwahashi T, Oide T, Hayashi R, Nakajima T, Ishikawa K, Mizusawa H	Spinocerebellar ataxia type 6 with motor neuron loss: A follow-up autopsy report.	J Neurol	294	633-635	2002
Miake H, Mizusawa H, Iwatsubo T, Hasegawa M	Biochemical characterization of the core structure of α- synuclein filaments.	J Biological Chemistry	277	19213-19219	2002
Kubodera T, Yokota T, Ohwada K, Ishikawa K, Miura H, Matsuoka T, Mizusawa H	Proteolytic cleavage and cellular toxicity of the human α1A calcium channel in spinocerebellar ataxia type 6 (SCA6).	Neuroscience Letters	341	74-78	2003
Li M, Ishikawa K, Toru S, Tomimitsu H, Takashima M, Goto J, Takiyama Y, Sasaki H, Imoto I, Inazawa J, Toda T, Kanazawa I, Mizusawa H.	Physical map and haplotype analysis of 16q-linked autosomal dominant cerebellar ataxia (ADCA) type III in Japan.	J Hum Genet	48	111-118	2003
常深泰司，水澤英洋	ポリグルタミン病―脊髄小脳失調症６型を中心に―	医学のあゆみ	201	1133-1142	2002
水澤英洋	核内封入体を伴わないポリグルタミン病	神経研究の進歩	46	637-645	2002
水澤英洋	Triplet repeat 病研究の進歩	組織培養工学	28	50-51	2002
融 衆太，水澤英洋	核封入体を作らないCAGリピート病 ―脊髄小脳失調症3型―	組織培養工学	28	11-14	2002

20020431

以降は雑誌/図書に掲載された論文となりますので、
「研究成果の刊行に関する一覧表」をご参照ください。

これ以降
PDF
なし

CHAPTER

6

Spinocerebellar Ataxia Type 4 (SCA4)

HIDEHIRO MIZUSAWA

Department of Neurology and Neurological Science
Graduate School, Tokyo Medical and Dental University
Tokyo, 113-8519 Japan

I. SUMMARY

SCA4 is a rare spinocerebellar ataxia characterized not only by cerebellar ataxia but also peripheral neuropathy and pyramidal tract involvement (Gardner *et al.,* 1994; Flanigan *et al.,* 1996). It was reported only in a large five-generation family of Scandinavian origin residing in Utah and Wyoming. The clinical manifestations include cerebellar ataxia such as ataxic gait, limb ataxia and dysarthria, loss of deep sensation and areflexia due to axonal sensory neuropathy, and occasional extensor plantar responses. The gene locus was mapped to chromosome 16q22.1. The same locus was demonstrated to show linkage in several Japanese families presenting with autosomal dominant pure cerebellar ataxia or cortical cerebellar atrophy (ADCCA). The 16q-linked ADCCA may be allelic to SCA4.

II. PHENOTYPE

SCA4 patients start to suffer from gait ataxia typically in the fourth or fifth decade with a median age at onset of 39.9 (19–59) years (Flanigan *et al.,* 1996). Gait disturbance is followed by difficulty in fine motor tasks and dysarthria. On examination, in addition to ataxic gait (95%) and limb dysmetria (95%), loss of vibration and joint-position sense (100%) as well as minimal loss of pinprick sense (95%) is frequently demonstrated. Ankle and knee-jerk are lost in almost all patients and complete areflexia is found in 25%. Extensor plantar response is seen in 20%. Distal limb weakness is reported in 4 and proximal as well as distal limb weakness is in 2 out of 20 patients. The patients showing weakness have positive Babinski's sign suggesting pyramidal tract involvement. Dysarthria is present in 50% and there are rare eye signs including saccadic pursuit and spontaneous lateral movements. Genetic anticipation is not very clear since the median age at onset is 41.9 years for the fourth generation and 36.7 years for the fifth generation. The phenomenon is observed in some families and not in other families. Differential diagnosis may include Friedreich ataxia because both diseases share possible dorsal column involvement and areflexia. Friedreich ataxia, however, is characterized by autosomal recessive inheritance, juvenile onset, and the presence of various extra-neural signs such as pes carvus, scoliosis, and cardiomyopathy. Other autosomal dominant ataxias including even SCA1, SCA2, Machado-Joseph disease, and SCA7 do not have such a severe sensory disturbance. Ataxias such as SCA5 and SCA6 show pure cerebellar ataxia which is very distinct from SCA 4 phenotype.

III. GENE LOCUS

The gene was reported to be tightly linked to the microsatellite marker D16S397 (lod score = 5.93 at theta = 0.00) in the 6-cM interval between D16S514 and D16S398.

IV. DIAGNOSTIC AND ANCILLARY TESTS

Sural nerve sensory response is absent in 12 out of 13 patients examined and radial sensory response is lost in 3. No reports on neuroimaging, cellular and animal models and treatment were available.

V. NEUROPATHOLOGY

The authors appeared to consider the phenotype of SCA4 similar to that of a French-German family with a late-onset ataxia and areflexia reported in 1954 (Biemond). In 1997, two sib cases with an SCA4 phenotype (Nachmanoff *et al.*, 1997) were also reported. These reports included autopsy findings in which the dorsal column and dorsal roots of the spinal cord as well as the cerebellar cortex were affected. However, there has been no definite evidence that the cases of Biemond or Nachmanoff were SCA4.

VI. ADCCA OR PURE CEREBELLAR ATAXIA LINKED TO SCA4 LOCUS

Recently a linkage study demonstrated many families of autosomal dominant pure cerebellar ataxia in Japan linked to a gene on SCA4 locus (Nagaoka, 2000). The gene locus was reported on 10.9 cM around D16S3107 (Fig. 6.1) which was later narrowed into 3.0 cM at the same region (Takashima *et al.*, 2001). The mean age at onset is 55.9 (45–72) years with mild genetic anticipation (the age at onset is 4.9 years younger in offspring). The initial symptom is gait ataxia followed by cerebellar dysarthria (92.6%), limb ataxia (92.6%), hypotonus (92.6%), and horizontal gaze nystagmus (63.0%). Except for a mild decrease in vibration sense in a very old patient with long duration of the illness, there are no sensory deficits. Tendon reflexes are almost normal except that only 16.6% of the patients have slightly decreased ankle-jerks. No pyramidal tract signs including Babinski's sign are observed.

Sensory and motor nerve conduction studies and EEG are normal in all the patients examined. Brain MRI reveals cerebellar atrophy without apparent involvement of the brainstem and other structures (Fig. 6.2). Therefore the phenotype is that of pure cerebellar ataxia or autosomal dominant cerebellar ataxia type III (ADCA-III) of Harding's classification (Harding, 1982) and completely different from that of SCA4 which is characterized by profound sensory disturbance and classified into Harding's ADCA-I. The 16q-linked ADCCA shares almost the same phenotype as SCA6 and is distinguished from SCA6 only by gene analysis. Identification of the causative gene would address the question whether the 16q-linked ADCCA and SCA4 are allelic or not.

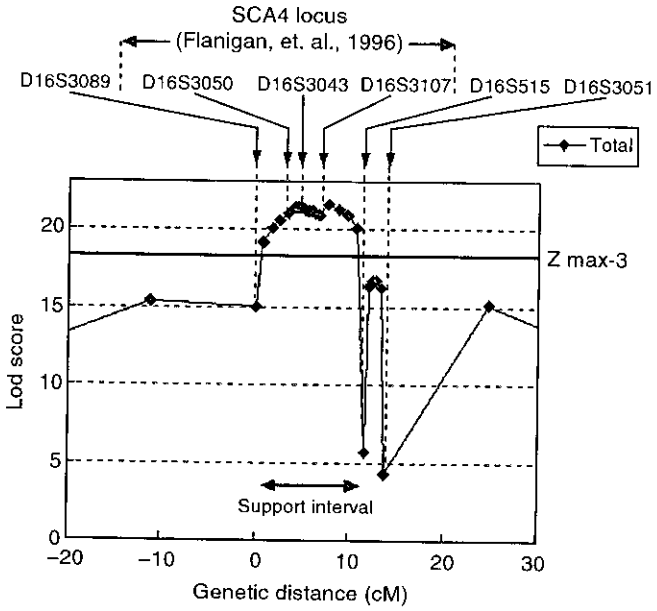

FIGURE 6.1 Multipoint lod scores of 16q-linked autosomal dominant pure cerebellar ataxia. The locus is supposed to be in the 10.9 cM region between 1.7 cM telomeric to D16S3089 and 1.3 cM centromeric to D16S515. The SCA4 locus lies in the region. (From Fig. 3, Nagaoka, U. *et al.*, (2000). *Neurology* 54, 1971–1975. With permission.)

FIGURE 6.2 Brain MRI of a patient with 16q-linked ADCCA. The cerebellum, particularly in the vermis, is atrophic but the pons is well preserved.

References

Biemond, A. (1954). La forme radiculo-cordonnale posteriure des degenerescences spinocerebelleuse. *Rev. Neurolog.* **91**, 2–21.

Flanigan, K., Gardner, K., Alderson, K., Galster, B., Otterud, B., Leppert, M. F., Kaplan, C., and Ptacek, L. J. (1996). Autosomal dominant spinocerebellar ataxia with sensory axonal neuropathy (SCA4): clinical description and genetic localization to chromosome 16q22.1. *Am. J. Hum. Genet.* **59(2)**, 392–399.

Gardner, K., Alderson, K., Galster, B., Kaplan, C., Leppert, M., Ptacek, L. (1994). Autosomal dominant spinocerebellar ataxia:Clinical description of a distinct hereditary ataxia and genetic localization to chromosome 16 (SCA4) in Utah kindred. *Neurology* **44**(Suppl.), 921S.

Harding, A. E. (1982). The clinical features and classification of the late onset autosomal dominant cerebellar ataxias. A study of 11 families, including descendants of "the Drew family of Walworth". *Brain* **105(Pt. 1)**, 1–28.

Nachmanoff, D. B., Segal, R. A., Dawson, D. M., Brown, R. B., and De Girolami, U. (1997). Hereditary ataxia with sensory neuronopathy: Biemond's ataxia. *Neurology* **48(1)**, 273–275.

Nagaoka, U., Takashima, M., Ishikawa, K., Yoshizawa, K., Yoshizawa, T., Ishikawa, M., Yamawaki, T., Shoji, S., and Mizusawa, H. (2000). A gene on SCA4 locus causes dominantly inherited pure cerebellar ataxia. *Neurology* **54(10)**, 1971–1975.

Takashima, M., Ishikawa, K., Nagaoka, U., Shoji, S., Mizusawa, H. (2001). A linkage disequilibrium at the candidate gene locus for 16q-linked autosomal dominant cerebellar ataxia type III in Japan. *J. Hum. Genet.* **46(4)**, 167–171.

Harding, A. E. (1982). The clinical features and classification of the late onset autosomal dominant cerebellar ataxias. A study of 11 families, including descendants of "the Drew family of Walworth". *Brain* **105(Pt. 1)**, 1–28.

THE JOURNAL OF BIOLOGICAL CHEMISTRY
Vol. 277, No. 9, Issue of March 1, pp. 7214–7221, 2002
Printed in U.S.A.

Novel $Ca_v2.1$ Splice Variants Isolated from Purkinje Cells Do Not Generate P-type Ca^{2+} Current*

Received for publication, August 27, 2001, and in revised form, December 11, 2001
Published, JBC Papers in Press, December 27, 2001, DOI 10.1074/jbc.M108222200

Taiji Tsunemi‡§¶, Hironao Saegusa‡¶, Kinya Ishikawa‡§¶, Shin Nagayama‡¶, Takayuki Murakoshi‡¶, Hidehiro Mizusawa§¶, and Tsutomu Tanabe‡¶‖

From the ‡Department of Pharmacology and Neurobiology and the §Department of Neurology and Neurological Science, Graduate School of Medicine, Tokyo Medical and Dental University, 1-5-45 Yushima, Bunkyo-ku, Tokyo 113-8519 and ¶Core Research for Evolutional Science and Technology, Japan Science and Technology Corp., Kawaguchi-shi, Saitama 332-0012, Japan

The $\alpha_1$2.1 (α_{1A}) subunits of P-type and Q-type Ca^{2+} channels are encoded by a single gene, *Cacna1a*. Although these channels differ in the inactivation kinetics and sensitivity to ω-agatoxin IVA, the mechanism underlying these differences remains to be clarified. Alternative splicings of the *Cacna1a* transcript have been postulated to contribute to the respective properties, however, the splice variants responsible for P-type Ca^{2+} channels have not been identified. To explore P-type-specific splice variants, we aimed at cloning $\alpha_1$2.1 from isolated mouse Purkinje cells using single-cell reverse transcription-PCR, because in Purkinje cells P-type currents dominate over the whole currents (>95%) with Q-type currents undetected. As a result, two novel splice variants were cloned. Compared with the previously cloned mouse $\alpha_1$2.1, two novel variants had additional 48 amino acids at the amino termini, six single amino acid changes, and splicing variations at the exon 46/47 boundary, which produced different carboxyl termini. Furthermore, one variant had one RNA editing site. However, electrophysiological and pharmacological studies indicated that these variants did not generate P-type current in cultured cells. These results suggest that P-type-specific splice variants may exist but that post-translational processing or modification by uncharacterized interacting proteins is also required for generating the P-type current.

Voltage-dependent Ca^{2+} channels (VDCCs)[1] have diverse functions and play important roles in many physiological activities such as secretion, contraction, migration, excitation, and gene expression (1, 2). VDCCs are composed of multiple subunits, designated α_1, β, $\alpha_2\delta$, and γ. Among them, the α_1 subunit is the largest and constitutes an ion-conduction pore, voltage sensor, and gating apparatus. Although the other auxiliary subunits modulate channel properties, the diversity of VDCCs comes primarily from the existence of multiple forms of the α_1 subunits. Electrophysiologically and pharmacologically, VDCCs are divided into six types (L, N, P, Q, R, and T), and ten genetically different cDNAs, which encode the α_1 subunit, have been identified. They are grouped into three families based on the similarities of deduced amino acid sequences (3). The Ca_v1 family ($Ca_v1.1$ through $Ca_v1.4$) includes channels containing α_{1S}, α_{1C}, α_{1D}, and α_{1F}, which constitute L-type Ca^{2+} channels. The Ca_v2 family ($Ca_v2.1$ through $Ca_v2.3$) includes channels containing α_{1A}, α_{1B}, and α_{1E}, which constitute P/Q-type, N-type, and R-type Ca^{2+} channels, respectively. The Ca_v3 family ($Ca_v3.1$ through $Ca_v3.3$) includes channels containing α_{1G}, α_{1H}, and α_{1I}, which mediate T-type Ca^{2+} currents. P/Q-type Ca^{2+} channels are expressed mainly in the central nervous system and contribute to neurotransmitter release (4–6). P-type Ca^{2+} channels were originally identified in cerebellar Purkinje cells (7), and Q-type Ca^{2+} channels were first described in cerebellar granule cells (8). Native P-and Q-type Ca^{2+} channels differ in inactivation kinetics and sensitivity to ω-agatoxin IVA (ω-Aga IVA) (8, 9). Recently, much attention has been paid to P/Q-type Ca^{2+} channels, because mutations in the $\alpha_1$2.1 subunit were reported to cause several neurological disorders such as familial hemiplegic migraine, episodic ataxia type 2, and spinocerebellar ataxia type 6 (SCA6) (10, 11). Clinically, SCA6 is characterized by pure progressive cerebellar ataxia (12). Pathologically, SCA6 is marked by the severe loss of Purkinje cells, where only P-type Ca^{2+} channels are expressed, and relatively intact cerebellar granule cells, where both P- and Q-type Ca^{2+} channels are expressed (13, 14). Although the relationship between P/Q-type Ca^{2+} channels' function and the pathophysiology underlying SCA6 has been extensively studied (15–17), the mechanisms relating Ca^{2+} channels' function to SCA6 are still unclear. To determine the relationship, it is important to elucidate the mechanism for the generation of P- and Q-type currents.

It has been hypothesized that the differences in the properties between P- and Q-type Ca^{2+} channels originate from alternative splicings of the pre-mRNA encoding $\alpha_1$2.1 subunit (1, 18). In fact, the *$Ca_v2.1$* gene encodes both P- and Q-type Ca^{2+} channels. This was confirmed by two recent findings: 1) antisense oligonucleotide blocked both P- and Q-type currents (19, 20); 2) both P- and Q-type currents were eliminated in $\alpha_1$2.1-deficient mice (21). Many $Ca_v2.1$ splice variants have been cloned by screening of mammalian cDNA libraries (11, 16, 18, 22). However, these variants have never shown native P-type-like currents when expressed in cultured cells (16, 18, 22, 24–26). One of the reasons why the possible P-type-specific splice variants have not been cloned may be that the amount of P-type splice variants is quite small in the cDNA libraries. It is difficult to obtain cDNAs from specific cells by screening of a conventional cDNA library, because it is made up of cDNAs

* The costs of publication of this article were defrayed in part by the payment of page charges. This article must therefore be hereby marked "*advertisement*" in accordance with 18 U.S.C. Section 1734 solely to indicate this fact.

The nucleotide sequence(s) reported in this paper has been submitted to the GenBank™/EBI Data Bank with accession number(s) AB066608 and AB066609.

‖ To whom correspondence should be addressed: Tel.: 81-3-5803-5167; Fax: 81-3-5803-0122; E-mail: t-tanabe.mphm@tmd.ac.jp.

[1] The abbreviations used are: VDCCs, voltage-dependent Ca^{2+} channels; ω-Aga IVA, ω-agatoxin IVA; SCA6, spinocerebellar ataxia type 6; RT, reverse transcription; ACSF, artificial cerebrospinal fluid; 3′-RACE, 3′ rapid amplification of cDNA end; nt, nucleotide(s); HEK, human embryonic kidney.

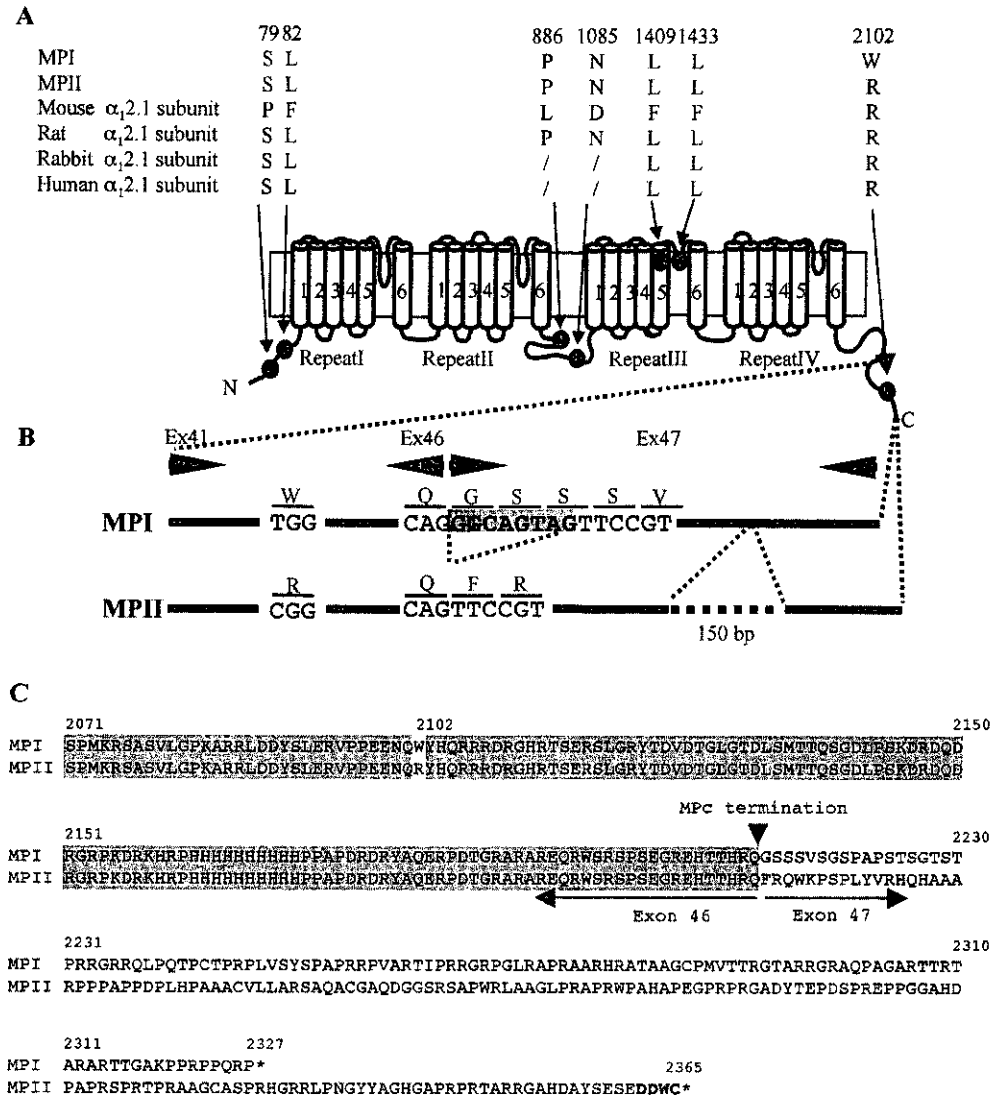

FIG. 1. **Novel splice variants of mouse $\alpha_1$2.1 subunit from Purkinje cells.** *A*, single amino acid substitution at six sites and one RNA editing site are indicated as *black dots* along the proposed topography of mouse $\alpha_1$2.1 subunit. These substitutions, including the RNA editing site, are compared among the sequences of previously reported mouse (30), rat (23), rabbit (22), and human (10, 11, 16) $\alpha_1$2.1 subunits. The *slashes* at amino acid positions 886 and 1085 indicate that corresponding amino acid sequences were not determined, because of the diverged sequences among mouse and other species. *B*, different exon 46/47 boundaries are shown for MPI and MPII. MPI contains a 5-bp (GGCAG) insertion prior to the TAG stop codon, and MPII lacks this TAG stop codon. This 8-bp difference leads to a translational frameshift in the exon 47. The exon numbers used in this figure are deduced from those of the human α_1*2.1* subunit gene (10), because the mouse α_1*2.1* gene structure has not been clarified yet. *C*, deduced carboxyl-terminal amino acid sequences of MPI and MPII. Identical amino acids between the two variants before exon 47 are *shaded*. RNA editing causes a single amino acid substitution from arginine (R) to tryptophan (W) at amino acid position 2102 in MPI. The coding region of MPc terminates at the position indicated by an *arrowhead*. *Asterisks* indicate stop codons. MPII has a terminal DDWC-COOH motif.

derived from heterogeneous cells. Recently single-cell reverse transcription-polymerase chain reaction (RT-PCR) was developed to investigate the expression of genes in a specific cell and has proven to be a useful tool for the identification of ion channel subunits (27, 28). In this study, we applied the single-cell RT-PCR to cloning of $\alpha_1$2.1 subunit from isolated mouse single Purkinje cells, where almost all the Ca^{2+} currents are P-type and no Q-type currents are recorded.

EXPERIMENTAL PROCEDURES

Preparation of RNA—C57BL/6N mice were anesthetized with methoxyflurane and decapitated, and the brains were quickly removed. Then cerebral cortices and cerebella were dissected. Total RNA was obtained from mouse cerebral cortices and cerebella using the standard acid guanidinium thiocyanate-phenol-chloroform extraction method (29).

Single Cell RT-PCR and Sequence Analysis—To obtain a single Purkinje cell or granule cells, a mouse cerebellum was cut into 300-μm slices in artificial cerebrospinal fluid (ACSF) saturated with 95% O_2-5% CO_2, and then the slices were incubated for 2 h at room temperature in the saturated ACSF to allow recovery from the injury due to slicing. The ACSF consisted of (in millimolar) 137 NaCl, 2.5 KCl, 0.58 NaH_2PO_4, 1.2 $MgCl_2$, 2.5 $CaCl_2$, 21 $NaHCO_3$, and 10 glucose. A single Purkinje cell was identified morphologically and then aspirated into a glass micropipette by applying negative pressure. Granule cells were also collected in a group using the same procedure. Aspirated single Purkinje cells or granule cells were directly expelled into thin-walled plastic tubes (PerkinElmer Life Sciences, Norwalk, CT) containing 5× First Strand buffer (4 μl), dNTP mixture (4 μl, 2.5 mM), RNase inhibitor (0.5 μl, 28,000 units/ml), dithiothreitol (2 μl, 0.1 M), and random hexamer (0.5 μl, 5 ng/μl) (PerkinElmer Life Sciences, Pomona, CA). The reaction mixture was incubated at 70 °C for 10 min and then placed on ice. SuperScript II reverse transcriptase (1 μl, 200 units/μl) (Invitrogen, Gaithersburg, MD) was added to the mixture, and then the reaction mixture was incubated at 25 °C for 10 min, 42 °C for 50 min, and 70 °C for 15 min. After the treatment, 1 μl of RNase H was added, and the sample was incubated at 37 °C for 15 min.

Primers were designed in reference to the sequence of the previously reported mouse $\alpha_1$2.1 cDNA (30) and of the 5′-upstream region of mouse $Ca_v2.1$ gene (31) (Table I). To discriminate PCR products derived from the genomic DNA, all the primer pairs were designed so that each primer was located in different exons. Nested PCR was carried out to

TABLE I
Primer sets

The exon numbers are deduced from those of human *CACNA1A* gene (10). The sequences which are exhibited as *bold letters* are added to the primers for subcloning.

Region, fragment size		Forward primer		Reverse primer	
		Primer name	Primer sequences (5′→3′)	Primer name	Primer sequences (5′→3′)
exon 1–6, 1001 bp	Outer primers	MaIA-5′-F1	ACAGCCCGGCCAGCCTGAGCA	MalA-R1	AGGAGATCAGTCCAGCCTTCCAT
	Inner primers	MaIA-5′-F2	**AAGCTT**TCGCCGCAGCAACAGCAGCCG	MalA-R2	CACTGGAAAACAGTGAGCACAGC
exon 6–12, 785 bp	Outer primers	MalA-F5	ACGACATCCAGGGTGAGTCGC	MalA-R5	AAGAGTGGAAGTAAGGCCGCGT
	Inner primers	MalA-F6	GACAGAGGAGCCTGCCCGCA	MalA-R6	AACATTTCGGACATAAAGAGTCCTAA
exon 11–19, 831 bp	Outer primers	MalA-F7	GGTCTCCCTTCGCCAGAGCCA	MalA-R7	ACGGCTATGGACATGTTGGCTG
	Inner primers	MalA-F8	TCACAAGAAGGAGAGAAGAATGCG	MalA-R8	TACCTCCTTGGCTTTCTGTAGAG
exon 16–25, 1806 bp	Outer primers	MalA-ex16-F2	TTTCAGATCCTGACTGGCGAAGAT	MalA-ex25R2	CTTCAGCTTTGGCAGCCGCTTG
	Inner primers	MalA-ex16-F1	CGGCATGGTGTTCTCCATCTA	MalA-ex25-R	AATGTCCTTTCCTTTGCTATTGCCA
exon 23–29, 997 bp	Outer primers	MalA-F13	TGCTGCGATATTTTGACTATGTTTTT	MalA-R13	GTACTCTTCCATCATCTTGTCTCC
	Inner primers	MalA-F14	CAGGCGTGTTTACCTTTGAGATG	MalA-R14	CTGAAAGGTGATGATGATCAAGGC
exon 28–36, 900 bp	Outer primers	MalA-F11	GGTCCTCAAGCACTCAGTGGAT	MalA-R11	CAGAAACGAGCACAGGAAGATGAA
	Inner primers	MalA-F12	CATGGAGATGTCCATCTTCTACGT	MalA-R12	GTTGCCGCAGTCTGCCGTGAG
exon 34–42, 959 bp	Outer primers	MalA-F9	GTGTTTGGCAACATCGGCATTGA	MalA-R9	AGGCATGTCGATGGGTGGCCC
	Inner primers	MalA-F10	GAGGATGAATTCCAAATCACGGAG	MalA-R10	GCTCCAGGTGCCAGTCTTCTG
exon 41–47, 1364/1506 bp	Outer primers	MalA-F3	AACCGGACACCACTCATGTTCCA	MalA-3′-R3	TAATAAGCTTGGCGTGGCCC
	Inner primers	MalA-F4	ATGGAGCCTCCATCACCAACACA	MalA-3′-R4	**TCTAGA**TAGCACTCCCGTGGGTCTGA
exon 41–46, 821 bp	Outer primers	MalA-F3	AACCGGACACCACTCATGTTCCA	MalA-3′-R3	TAATAAGCTTGGCGTGGCCC
	Inner primers	MalA-F4	ATGGAGCCTCCATCACCAACACA	MalA-R4	**TCTAGA**CTACTGTCTGTGTGT

amplify $\alpha_1$2.1 cDNA from single Purkinje cells. Single-cell cDNA (2.5 μl) was used as a template for the first PCR amplification. The reaction mixture contained: PCR-grade H_2O (7.5 μl), 5× Advantage-GC PCR Buffer (5 μl), dNTP mixture (2.5 μl, 2.5 mM), GC Melt (2.5 μl, 5 M), each primer (2 μl, 2.5 μM), and 50× Advantage-GC cDNA polymerase mix (1 μl) (CLONTECH, Palo Alto, CA). The thermal cycling program for the first PCR was 35 cycles of 96 °C for 4 min, 60 °C (56 °C for some primers) for 1 min, and 72 °C for 3 min. The first PCR product (2.5 μl) was used as a template for the second PCR. The reaction mixture contained: PCR-grade H_2O (10 μl), 10× Cloned *Pfu* DNA polymerase reaction buffer (2.5 μl), dimethyl sulfoxide (2.5 μl), dNTP mixture (2.5 μl, 2.5 mM), each primer (2 μl, 2.5 μM), and *PfuTurbo* DNA polymerase (1 μl, 2.5 units/μl) (Stratagene, La Jolla, CA). The second PCR program was the same as the first except that the number of PCR cycles was 20 or 25. To obtain the 3′-downstream region, 3′ rapid amplification of cDNA end (3′-RACE) was performed initially with 1 μg of poly(A)$^+$ RNA from mouse cerebellum using a Marathon cDNA amplification kit (CLONTECH) according to the manufacturer's instructions. The reaction products were subcloned into pCR 2.1 (Invitrogen, San Diego, CA) and sequenced using an ABI Prism 310 genetic analyzer (PerkinElmer Life Sciences). Then reverse primers were designed so that they were located downstream from the termination codons of any reading frames (Ma1A3′R3 and Ma1A3′R4; Table I). With these primers, nested PCR was also performed with a single Purkinje cell as described above. All PCR products were gel-purified and subcloned into the *Hinc*II site of pUC18 and sequenced. We used two independent Purkinje cells to avoid possible PCR errors.

Expression Vectors—Eight independent nested PCR reactions were designed so that the resulting PCR products covered the entire coding region of the mouse $\alpha_1$2.1 subunit. The adjacent PCR products possessed overlapping sequences in which unique restriction sites occurred, making it easy to connect all the fragments to construct expression vectors (pcDNAI/Amp, Invitrogen, was used as the backbone vector). With regard to the most 3′ region, two fragments with different sizes (1364 and 1506 bp) were amplified (Table I). The $\alpha_1$2.1 with the shorter 3′ sequence was designed MPI and the longer MPII. Thus, MPI and MPII differed only in their 3′ sequence corresponding to the exon 41–47 (Fig. 1*C*).

PKCRα2 and PKCRβ that encode $\alpha_2\delta$ and β_{1a} subunits, respectively, were described previously (32). The expression vector for the β_{2a} or β_3 subunit was constructed by subcloning the inserted fragment of pBH19 or pBH23 (33) into pKCRH2 (34), respectively. The expression vector for the β_4 subunit was constructed by subcloning the inserted fragment of β k213 (35) into pcDNAI/Amp.

Construction of MPc—We also constructed a plasmid carrying the mouse $\alpha_1$2.1 whose coding region terminated in the end of exon 46 and designated this version of $\alpha_1$2.1 as MPc. A stop codon (TAG) was artificially introduced immediately after the end of exon 46 by PCR using MPII as a template and primer MalAF4 and MalAR4 (Table I) as a mutagenic primer. Then MPc was constructed by connecting the artificially made exon 41–46 fragment together with the seven same fragments that were used to construct MPI or MPII.

Colony Hybridization for Detection of RNA Editing Events—Fragments with a size of 780 bp containing nucleotide (nt) 6358 were PCR-amplified from cDNAs that were prepared from single Purkinje cells, cerebellar granule cells, or cerebral cortex. The primers used were Ma1A-F4 (Table I) as a forward primer and MalA-RE (5′-TGGGC-GAGCGGGACCAGCG-3′) as a reverse primer. Each PCR product was subjected to both direct sequencing and subcloning into pCR 2.1. For control experiments, we used two plasmids that contained the exon 41–47 fragment of MPI and MPII. The *Escherichia coli* colonies were transferred to nylon membranes (Hybond-N+, Amersham Biosciences, Inc., Uppsala, Sweden). The membranes were hybridized with 18-mer oligonucleotide probe 6358C (5′-AGAACCAACGGTACCACC-3′) or 6358T (5′-AGAACCAATGGTACCACC-3′). The probes were ^{32}P-end-labeled using [γ-^{32}P]ATP (>5000 Ci/mmol) and T4 polynucleotide kinase (New England BioLabs, Beverly, MA). Hybridization was performed at 37 °C for 16 h in 4× SSC containing 0.1% SDS, 1× Denhardt's reagent, and 50 μg/ml herring sperm DNA (Roche Molecular Biochemicals, Mannheim, Germany). After hybridization, the membranes were washed in 1× SSC with 0.1% SDS at 37 °C for 20 min. Autoradiography was performed with Hyperfilm-ECL (Amersham Biosciences, Inc.) at −80 °C using an intensifying screen.

Cell Culture and Transfection—The procedures of cell culture and transfection were the same as those previously described (16). In brief, human embryonic kidney (HEK) 293 cells were grown in Dulbecco's modified Eagle's medium/F-12 medium (Invitrogen) supplemented with 10% fetal bovine serum (Invitrogen) and 50 μg/ml gentamicin (Invitrogen). The $\alpha_1$2.1 subunits were transiently co-expressed with $\alpha_2\delta$ and one of the β subunits, and pEGFP-C2 (CLONTECH) was used as a transfection marker. Transfection was performed with a calcium phosphate precipitation method (Mammalian Transfection kit, Stratagene). Electrophysiological analysis was performed 36–72 h after transfection.

Whole-cell Recordings—Patch pipettes were pulled from borosilicate glass (GC150F-4, Warner, Instruments, Hamden, CT) and filled with a solution consisting of (in millimolar) 140 CsCl, 2 $MgCl_2$, 10 EGTA, 10 HEPES, 3 ATP·Mg (pH 7.4 with CsOH). Pipette resistance ranged from 2 to 4 MΩ. The external solution consists of (in millimolar) 15 $BaCl_2$,

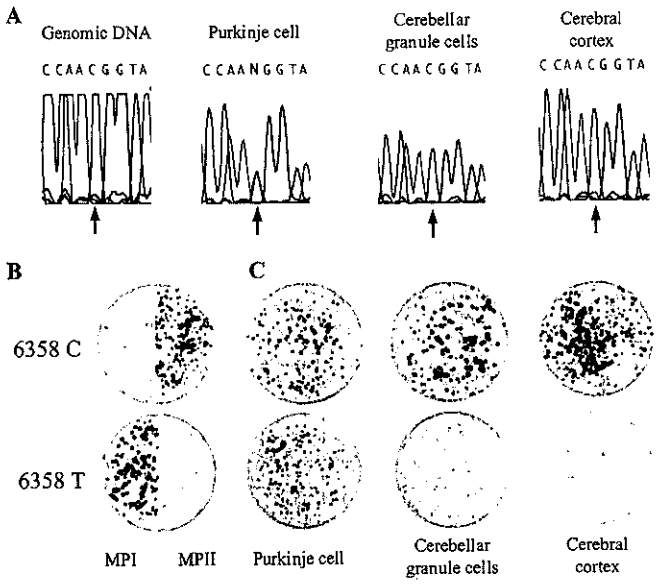

FIG. 2. **Nucleotide sequence and colony hybridization analyses to detect RNA editing in mouse $\alpha_1$2.1 subunit in Purkinje cells.** *A*, direct sequencing of the PCR fragments, which were amplified from mouse genomic DNA and cDNAs prepared from Purkinje cells, cerebellar granule cells, or cerebral cortex. The nucleotide position 6358 is indicated by *arrows*. *B*, control hybridization experiments to show the specificity of the probes. Colonies containing the PCR fragments of MPI are shown in the *left half* of each membrane, and colonies containing the PCR fragments of MPII are shown in the *right half*. The *upper membrane* was hybridized with probe 6358C, and the *lower* with probe 6358T. Colonies containing the PCR fragments of MPI and MPII show clearly different hybridization patterns with probes 6358C and 6358T. *C*, cell specificity of the RNA editing. Probes 6358C and 6358T hybridize with about the same number of colonies containing the PCR fragments, which were amplified from cDNA from Purkinje cells (*left*). In contrast, probe 6358C but not 6358T hybridizes specifically with the colonies containing the PCR fragments of cerebellar granule cells (*center*), or cerebral cortex (*right*).

145 tetraethylammonium chloride, 10 HEPES, and 10 glucose (pH 7.4 with tetraethylammonium-OH). Barium currents were recorded at room temperature (22–25 °C) under a whole-cell mode of the patch clamp recording with an amplifier (EPC-9, HEKA, Lambrecht/Pfalz, Germany). The holding potential was −80 mV unless otherwise stated. Series resistance was electronically compensated by 50–80%. All illustrated and analyzed currents were corrected for remaining capacitance and leakage currents using the −P/4 method. Data were filtered at 3 kHz (four-pole Bessel filter) and sampled at 10 kHz. The software (Pulse+PulseFit 8.09, HEKA) was used for data acquisition and analysis. In the experiments with ω-Aga IVA (Peptide Institute, Inc., Osaka, Japan), the external solution was supplemented with 0.1 mg/ml cytochrome *c* to prevent nonspecific binding of the toxin.

Statistical Analysis—All data were presented as mean ± S.E. Statistical analysis was performed using an unpaired Student's *t* test.

RESULTS

Cloning of Novel Mouse $\alpha_1$2.1 Subunit Variants—We cloned two novel splice variants of $\alpha_1$2.1 subunit from the mouse Purkinje cell using the single-cell RT-PCR technique. Compared with the sequences of rabbit $\alpha_1$2.1 subunit (BI-1) or rat $\alpha_1$2.1 (rbA-1), the previously reported mouse $\alpha_1$2.1 lacked 46 or 48 amino acids in the amino terminus, respectively (30). However, $\alpha_1$2.1 variants we cloned in this study commonly contained the 5′ sequences homologous to those of BI-1 and rbA-1, suggesting that the amino termini of our newly cloned $\alpha_1$2.1 variants are longer by 48 amino acid residues than that of the previously reported mouse $\alpha_1$2.1. Together with this difference, two novel $\alpha_1$2.1 had single base substitutions at 16 sites located from exon 1 to exon 41 compared with the previously reported mouse $\alpha_1$2.1. We confirmed these 16 single base substitutions in two independent Purkinje cells. Therefore, PCR errors are unlikely to be the cause of the substitutions. Ten of the 16 substitutions were silent polymorphisms leading to no amino acid changes, and the rest of them resulted in amino acid changes. Two altered amino acids found in II–III loop (L886P, D1085N) were identical to the sequence of rbA-1, and the remaining four found in repeat I (P79S, F82L) and repeat III (F1409L, F1433L) were conserved in BI-1, rbA-1, and human $\alpha_1$2.1 subunit (Fig. 1*A*).

In the human *$Ca_v2.1$* gene, differential splice acceptor usage at the boundary of intron 46/exon 47 is known to yield an $\alpha_1$2.1 variant with a longer carboxyl terminus (11), because the stop codon in the beginning of exon 47 was no longer in-frame. The same kind of variant was also found in rat $\alpha_1$2.1 (36). But the nucleotide sequence of mouse $\alpha_1$2.1 corresponding to the variant with a longer carboxyl-tail has not been reported so far. This carboxyl-terminal sequence, which is thought to be encoded by exon 47, is expressed abundantly in rat Purkinje cell bodies and dendrites as revealed by an immunohistochemical study (17) and may affect channel properties. Therefore, we tried to clone the mouse exon 47 by 3′-RACE. Because a single Purkinje cell has an extremely small amount of RNA, it is expected to be difficult to apply 3′-RACE. Therefore, we first applied 3′-RACE to mouse cerebellar poly(A)$^+$ RNA. As a result, a novel fragment with a size of 1504 bp was cloned, and sequence analysis revealed that there were termination codons in all the reading frames on the sequence. Then we designed reverse primers (Ma1A-3′-R3, Ma1A-3′-R4; Table I) to perform RT-PCR with single Purkinje cells. Two fragments with different sizes of 1364 and 1506 bp were amplified. We assigned the novel $\alpha_1$2.1 with the shorter fragment MPI, and the $\alpha_1$2.1 with the longer fragment MPII. The nucleotide sequences of MPI and MPII were completely the same except for these most 3′ sequences, where several distinctive features were found in the two variants (Fig. 1, *B* and *C*). First, a single nucleotide conversion (C to T) was observed at nt 6358 in MPI. This conversion led to an amino acid substitution from arginine to tryptophan (Fig. 1, *B* and *C*). Second, there were two variations at the beginning of exon 47. In MPI, 5 nucleotide residues (GGCAG) were inserted, whereas in MPII 3 nucleotide residues (TAG) were deleted, when compared with the previously published sequence (30) (Fig. 1*B*). These 5-bp insertion and 3-bp deletion steps resulted in different reading frames in exon 47. It may be worth noting that the previously reported variant was cloned from cerebellar cDNA but not from Purkinje cell cDNA. Third, in MPI, a 150-bp sequence corresponding to nt 6831–6980 in MPII was deleted (Fig. 1*B*). The 3′ sequence of the MPII (nt 6691–7149) was identical to the corresponding mouse genomic sequences (GenBank™ accession number AC079509), suggesting that this region was encoded by a single exon. This also suggests that the 150-bp deletion in MPI was caused by an alternative splicing. Finally, carboxyl-terminal sequences are different. MPII has an evolutionarily conserved sequence (DDWC-COOH) at the carboxyl terminus but MPI does not have this sequence (Fig. 1*C*).

Sequence analysis of MPI and MPII revealed an open reading frame of 6981 and 7095 nucleotides encoding a protein of 2327 and 2365 amino acid residues, respectively. Except for the exon 47 sequences, deduced amino acid sequences of MPI and MPII were 89%, 91%, and 99% identical to those of BI-1 (22), human $\alpha_1$2.1 (16), and rbA-1 (23), respectively.

RNA Editing in the $\alpha_1$2.1 Subunit Occurred Specifically in Purkinje Cells—Sequence analysis of genomic DNA revealed that the nucleotide corresponding to position 6358 of the cDNA was C (Fig. 2*A*), therefore, the cytidine-to-uridine (C-to-T in cDNA) conversion in MPI was thought to be due to RNA editing. We then directly sequenced cDNA fragments containing this region, which were prepared from single Purkinje cells,

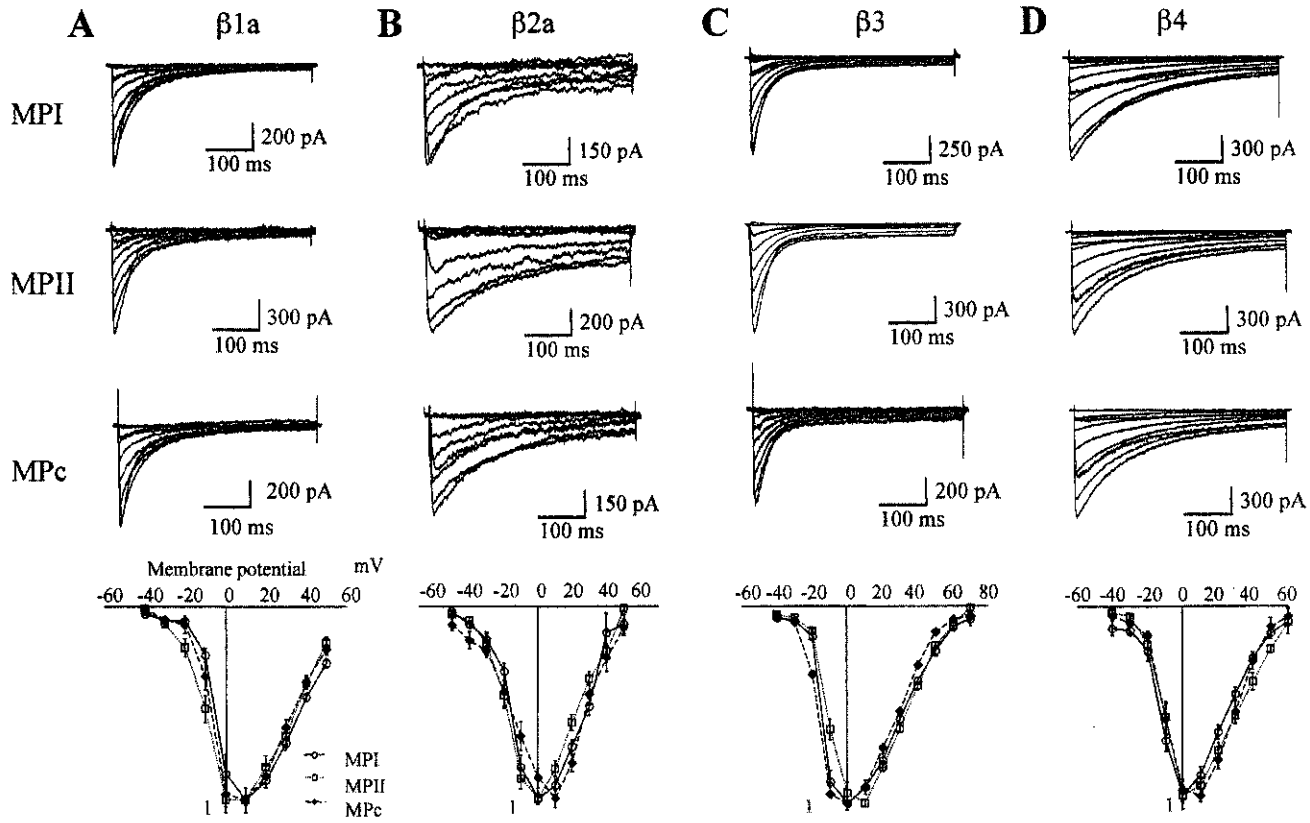

FIG. 3. **Normalized current-voltage relationships in MPI, MPII, and MPc channels.** Barium current was elicited by 400-ms depolarizing pulses from a holding potential of −80 mV to test potentials (−40 mV to 70 mV) with an increment of 10 mV. Representative current traces of MPI (*top*), MPII (*upper middle*), and MPc (*lower middle*) co-expressed with β_{1a} (*A*), β_{2a} (*B*), β_3 (*C*), and β_4 (*D*) subunits. Normalized current-voltage relationships are shown in the *bottom row*. MPI (*open circle*), MPII (*open square*), and MPc (*closed diamond*) were co-expressed with β_{1a} (n = 20, 24, 24, respectively), β_{2a} (n = 12, 11, 9, respectively), β_3 (n = 14, 10, 8, respectively), or β_4 (n = 7, 10, 8, respectively).

granule cells, or cerebral cortex. The sequence analysis revealed that nucleotide position 6358 is C in granule cells and cerebral cortex. On the other hand, in Purkinje cells, sequence analysis at the same position displayed N, suggesting that C and T were simultaneously exhibited (Fig. 2*A*). Then colony hybridization was performed to confirm the specificity and efficiency of this conversion. In control experiments, autoradiograms of representative hybridization with the ^{32}P-end-labeled oligonucleotide probes, 6358C and 6358T, sharply discriminated the colonies carrying plasmids, which contained the exon 41–47 fragment of MPI and that of MPII (Fig. 2*B*). As for the experiment with Purkinje cells, the number of colonies hybridizing with the probe 6358C and 6358T was almost the same. By contrast, no hybridization of the probe 6358T occurred in the experiments with cerebellar granule cells or cerebral cortex (Fig. 2*C*). These results suggest that C-to-T conversion occurred specifically and in approximately half of the $Ca_v2.1$ mRNA in this Purkinje cell.

Electrophysiological and Pharmacological Studies of MPI, MPII, and MPc Channels Expressed in HEK293 Cells—MPI, MPII, or MPc was expressed together with $\alpha_2\delta$ and one of the four β subunits (β_{1a}, β_{2a}, β_3, and β_4) in HEK293 cells, and the electrophysiological properties were studied with a whole-cell patch-clamp technique. Because functional properties of the previously cloned mouse $\alpha_1$2.1 were not reported, we needed a control mouse $\alpha_1$2.1 to investigate how the carboxyl termini of MPI and MPII influence channel properties. To this end, we constructed MPc whose coding region was terminated in the end of exon 46. Expression plasmids encoding this version of $\alpha_1$2.1 of other species have been used for many electrophysiological studies (18, 22, 25, 26, 28, 41). Although MPc as well as MPI and MPII contained six single amino acid changes from exon 1 to exon 41 compared with the sequence of the previously cloned mouse $\alpha_1$2.1, the changed amino acids were conserved among the $\alpha_1$2.1 cloned from other species (Fig. 1*A*). Therefore, these amino acid changes were supposed to affect the channel properties little. In fact, the current recorded from the MPc channel was similar to those recorded from the channels containing $\alpha_1$2.1 of other species (Fig. 3).

Barium currents were elicited by 400-ms depolarizing test pulses from a holding potential of −80 mV to test potential (−40 to +50 mV) in 15 mM Ba^{2+} solutions. Whole-cell Ba^{2+} currents recorded in HEK293 expressing MPI, MPII, or MPc were almost the same. Although β subunits were reported to significantly influence Ca^{2+} channel properties, we were not able to record precise P-type currents from the cells expressing any combinations of $\alpha_1$2.1 and β subunits (Fig. 3, *A–D*). All channels were activated at a test potential of −20 mV, and the currents gradually developed to maximal amplitude at about 20 mV. Normalized current-voltage curves were not significantly different among MPI, MPII, and MPc. To compare the activation kinetics, we quantified the time course by fitting the currents to single-exponential function. To compare the inactivation kinetics, we quantified the time course by fitting the currents to double-exponential function in β_{1a}-associated channels and single-exponential function in the other channels. The obtained time constants for activation and inactivation at 20 mV are shown in Table II. They were not significantly different among these channels. Next, the voltage dependence of activation for the expressed Ca^{2+} channels was compared (Fig. 4 and Table III). Conductance was calculated from the peak current. The normalized values of conductance were then fitted to a single Boltzmann function. The half-maximal voltage of activation ($V_{1/2}$), the slope factor (k), and the percent decaying were

TABLE II

Activation and inactivation kinetics of MPI, MPII, and MPc in HEK293 cells at 20 mV

Values are means ± S.E., n, number of cells recorded; τ_{act}, time constants for activation; τ_{fast} and τ_{slow}, fast and slow time constants for inactivation. Activation kinetics were derived by fitting a single exponential function: $I_{Ca} = I_S[1 - \exp(-t/\tau_{act})]$, where I_{Ca} is the total current, and I_S is the steady-state current, to the activating segment of test currents. Inactivation kinetics were obtained by fitting single- or double-exponential functions: $I_{Ca} = -I_{intact} - \exp(-t/\tau_{slow}) - NI$ or $I_{Ca} = -I_{fast} \cdot \exp(-t/\tau_{fast}) - I_{slow} \cdot \exp(-t/\tau_{slow}) - NI$, respectively; I_{inact}, total inactivation component of the total current, I_{fast} and I_{slow}, the fast and slow inactivation component of the total current; NI, the noninactivating component of the total current.

β subunit	$\alpha_1$2.1	n	Activation	Inactivation	
			τ_{act}	τ_{fast}	τ_{slow}
				ms	
β1a	MPI	12	1.20 ± 0.08	29.4 ± 2.7	132.7 ± 13.7
	MPII	10	1.17 ± 0.17	29.1 ± 2.1	128.2 ± 14.8
	MPc	10	1.10 ± 0.17	32.3 ± 1.8	129.2 ± 14.6
β2a	MPI	12	4.19 ± 0.06		70.2 ± 5.2
	MPII	9	4.57 ± 0.07		69.4 ± 4.2
	MPc	7	4.21 ± 0.12		65.3 ± 7.7
β3	MPI	10	1.14 ± 0.05		42.0 ± 3.5
	MPII	9	1.21 ± 0.05		42.5 ± 4.3
	MPc	7	1.08 ± 0.03		38.6 ± 3.5
β4	MPI	5	1.70 ± 0.16		142.1 ± 11.7
	MPII	9	1.61 ± 0.15		155.0 ± 14.8
	MPc	6	1.80 ± 0.15		163.8 ± 14.0

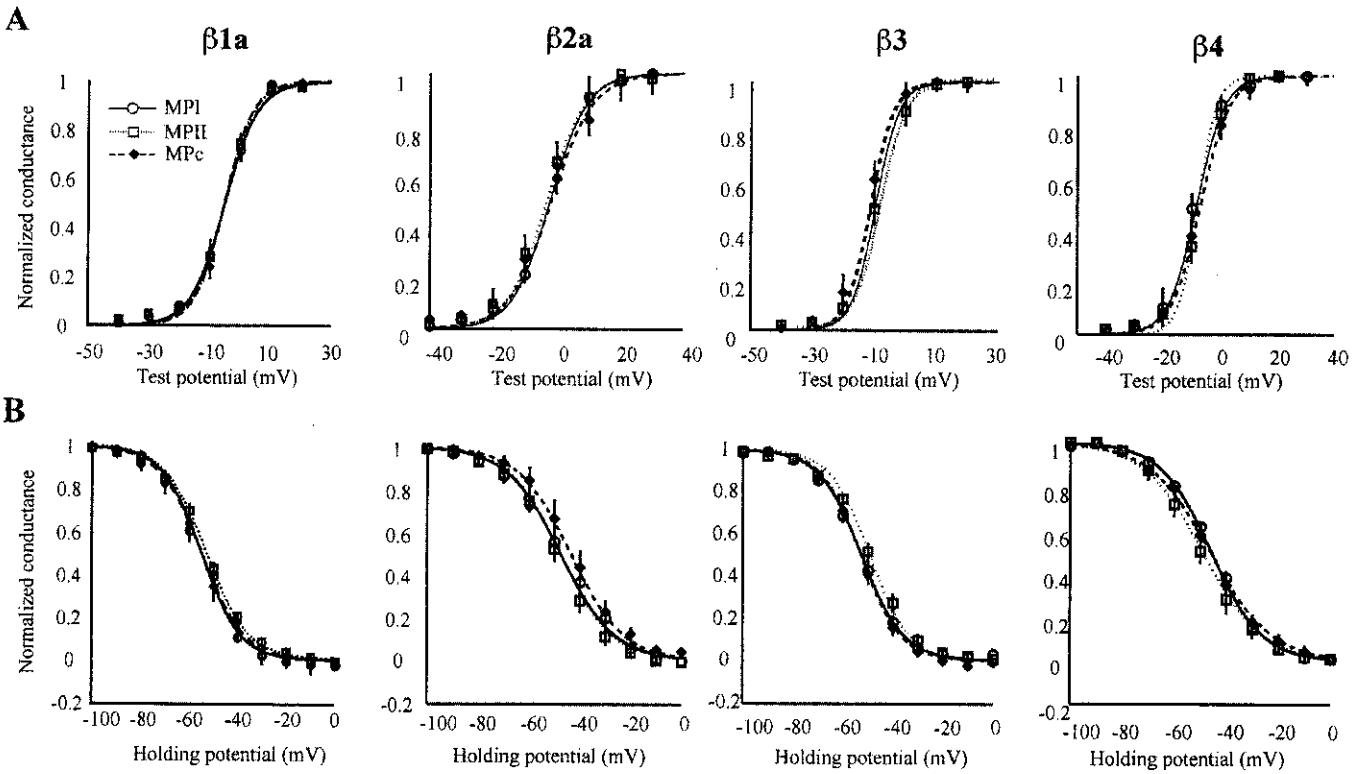

FIG. 4. **Voltage dependence of activation and inactivation of MPI, MPII, and MPc expressed in HEK293 cells.** *A*, voltage dependence of activation. Activation was estimated by relative conductance (G_{Ca}/G_{Ca}max). Values of conductance (G_{Ca}) were calculated as $G_{Ca} = I_{Ca}/(V_m - V_{rev})$, where I_{Ca} and V_{rev} were the peak current for the test potential (V_m), and the reversal potential, respectively. The V_{rev} value was obtained from peak $I_{Ca} - V_m$ data. Mean normalized conductances were plotted against test potentials and fitted to the Boltzmann equation. MPI, *open circle*; MPII, *open square*; MPc, *closed diamond* with β_{1a} (n = 20, 12, 14, respectively), β_{2a} (n = 12, 9, 7, respectively), β_3 (n = 9, 8, 7, respectively), β_4 (n = 5, 10, 6, respectively). *B*, Voltage dependence of inactivation. Currents were elicited by a two-pulse protocol: a 2-s conditioning prepulse (voltage ranging from −100 to 0 mV with a 10-mV increment) was given before 50-ms test pulse (20 mV). The values of current amplitude normalized by the maximum amplitude in the series were plotted against potentials of the conditioning prepulse. Means ± S.E. were obtained from MPI, MPII, and MPc channels under the presence of β_{1a} (n = 9, 10, 10, respectively), β_{2a} (n = 9, 11, 7, respectively), β_3 (n = 11, 10, 8, respectively), or β_4 (n = 7, 10, 6, respectively).

not different among the channels. Compared with β_{1a}- and β_3-associated channels, β_{2a}- and β_4-associated ones demonstrated slower inactivation currents. However, they were still faster than P-type current, which does not decay over 1 s (37). A two-pulse protocol was applied to examine the voltage dependence of inactivation. To reach a steady state, a 2-s prepulse (from −100 to 0 mV with a 10-mV increment) preceded a test pulse of 20 mV. The values of normalized current amplitude were plotted against holding potentials (Fig. 4). The $V_{½}$ and k were not significantly different among the channels (Table III).

The major pharmacological difference between P- and Q-type Ca^{2+} channels is the sensitivity to the spider peptide toxin,

TABLE III

Parameters of voltage dependence of activation and inactivation of MPI, MPII, and MPc in HEK293 cells

Values are means ± S.E. n, number of cells recorded; $V_{½}$, half-maximal voltage of activation and inactivation: k, slope factor. Data were fitted with a single Boltzmann function: $G_{Ca}/G_{max} = \{1 + \exp[-(V_m - V_{½})/k]\}^{-1}$ for activation, $I_{Ca}/I_{max} = \{1 + \exp[(V_m - V_{½})/k]\}^{-1}$ for inactivation, where G_{Ca}/G_{max} is the relative conductance, I_{Ca}/I_{max}, the relative current and V_m, membrane potential. Percent decay is defined as $100 \times (I_{peak} - I_{at\ 400\ ms})/I_{peak}$.

β subunit	$\alpha_1$2.1	n	Activation			Inactivation		
			$V_{½}$	k	Percent decay	n	$V_{½}$	k
			mV		%		*mV*	
β1a	MPI	11	−5.8 ± 0.8	5.7 ± 0.7	95.1 ± 1.8	9	−55.0 ± 2.4	7.1 ± 0.9
	MPII	10	−5.0 ± 0.7	5.7 ± 0.7	93.9 ± 1.3	10	−57.0 ± 1.4	7.8 ± 1.9
	MPc	11	−5.3 ± 0.7	5.4 ± 0.3	95.1 ± 1.2	14	−56.2 ± 1.6	7.0 ± 0.5
β2a	MPI	12	−1.7 ± 0.4	6.3 ± 0.8	76.9 ± 2.2	9	−47.3 ± 3.0	10.6 ± 0.5
	MPII	9	−2.2 ± 0.6	5.8 ± 1.3	74.8 ± 3.4	11	−47.5 ± 1.7	10.1 ± 1.0
	MPc	7	−1.7 ± 0.2	6.5 ± 0.8	77.1 ± 4.7	7	−43.3 ± 3.5	10.4 ± 0.7
β3	MPI	9	−9.8 ± 1.6	3.8 ± 0.4	88.8 ± 1.5	11	−52.3 ± 1.4	8.5 ± 0.3
	MPII	8	−8.1 ± 1.4	4.1 ± 0.4	88.1 ± 2.7	10	−49.0 ± 3.0	8.9 ± 0.5
	MPc	7	−11.1 ± 1.9	3.7 ± 0.6	90.7 ± 1.5	8	−52.4 ± 1.2	7.9 ± 0.6
β4	MPI	5	−8.3 ± 0.4	4.8 ± 0.8	79.0 ± 2.5	7	−47.3 ± 3.0	10.6 ± 0.5
	MPII	10	−8.0 ± 0.4	4.3 ± 0.8	81.7 ± 2.2	10	−47.3 ± 3.0	10.6 ± 0.5
	MPc	6	−6.9 ± 1.0	5.0 ± 0.7	80.2 ± 3.4	6	−46.1 ± 1.0	11.0 ± 0.2

ω-Aga IVA. Co-expression studies with different β subunits revealed that β_1-associated channels exhibit high affinity to this toxin (38). Therefore, we chose the β_{1a} subunit for this study. The currents mediated by MPI, MPII, and MPc channels were half-blocked by 50 nM ω-Aga IVA (Fig. 5). This sensitivity was close to that of Q-type Ca^{2+} channels previously described (8).

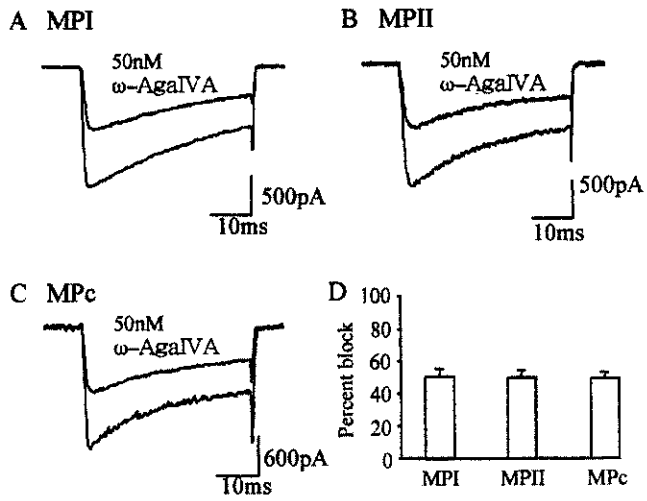

FIG. 5. **ω-Aga IVA sensitivity of MPI, MPII, and MPc transiently expressed in HEK293 cells with β_{1a} subunit.** *A–C*, whole-cell currents obtained from MPI (*A*), MPII (*B*), and MPc (*C*) before and 10 min after application of 50 nM ω-Aga IVA. Barium currents were elicited by 50-ms depolarization pulses to 20 mV from a holding potential of −80 mV. *D*, comparison of 50 nM ω-Aga IVA sensitivity. Means ± S.E. were obtained from MPI (n = 3), MPII (n = 4), and MPc (n = 3).

DISCUSSION

In this study, we have cloned two novel mouse $\alpha_1$2.1 variants, MPI and MPII, carrying different 3′ sequences. There are several distinctive features between the two variants.

First, a single base substitution at nt 6358 (C or T) is likely caused by RNA editing, because sequence analysis of genomic DNA corresponding to this region revealed C. Interestingly, this conversion occurred specifically in Purkinje cells as far as examined and the efficiencies were variable among Purkinje cells. In some cells, the efficiencies reached to 50%, in other cells, efficiencies were very low (data not shown). These results suggest that MPI, which has this C-to-T conversion, is expressed specifically in Purkinje cells with different abundance. RNA editing is a post-transcriptional modification that results in generation of nucleotides within an RNA transcript that are different from the sequence of the genome. RNA editing may have profound functional consequences in protein functions. For example, the adenosine-to-inosine (A-to-I) conversion within the RNA encoding the GluR-B subunit of α-amino-3-hydroxy-5-methyl-4-isoxazole propionic acid-subtype glutamate receptors (Q/R site) alters calcium permeability (39). Although channel properties of MPI, which contains an RNA-edited site, were not different from those of MPc in the heterologous expression system, the cell specificity of the editing event would suggest important roles of this variant in Purkinje cells.

Second, the two variants differed at the beginning of exon 47, presumably due to different splice acceptor usage. It is known that there are sequence variations at the boundary of exon 46/47 in $\alpha_1$2.1 mRNA: two variations with and without GGCAG insertion before the TAG stop codon located at the beginning of exon 47 have been reported in human and rat $\alpha_1$2.1 (11, 26). MPI seems to correspond to the human and rat version possessing the GGCAG insertion, however, MPI has the deduced amino acid sequence diverged from these variants. We have cloned another variant, MPII, in which the TAG stop codon is deleted and carboxyl terminus is extended with different reading frame from that of MPI. Thus, we have identified only the carboxyl-terminal extended versions of $\alpha_1$2.1 in mouse Purkinje cells. An immunohistochemical study revealed that the exon 47 sequence, with the same reading frame as MPI, is expressed intensely in Purkinje cells (17). Interestingly, however, the $\alpha_1$2.1 in which the coding region is terminated in the end of exon 46 was cloned from a cerebellar cDNA library, suggesting that these variants for $\alpha_1$2.1 are expressed in different cell populations in the cerebellum.

Third, as mentioned, MPI and MPII have different carboxyl-terminal sequences. In MPII, there is an evolutionarily conserved sequence at the carboxyl-tail: DDWC-COOH. This (E/D)XWC-COOH motif is conserved in the wide range of animals from *Drosophila* to human. This suggests that this motif has important biochemical roles. Indeed, it is known that this motif is specifically recognized by the PDZ domain of Mint1, which in association with CASK and Ca^{2+} channel can modulate synaptic vesicle fusion and neurotransmitter release (40). Therefore, MPI, which does not have this motif, and MPII might have distinct functions in the control of synaptic transmission.

Taken together, our results suggest that MPI and MPII are

differently localized in cerebellar cells with different functions. Therefore, we then investigated the channel properties of MPI, MPII, and MPc. It was reported that β subunits were influential on the Ca^{2+} channel properties (38, 41); however, P-type-associated β subunit has not yet been identified. Therefore, we expressed MPI, MPII, or MPc with one of the various β subunits in HEK293 cells and compared their channel properties.

As a result, the characteristics of MPI, MPII, and MPc were not significantly different, suggesting that the alternatively spliced form of $\alpha_1$2.1 identified in Purkinje cells by itself is not sufficient to generate P-type current when expressed in combination of β and $\alpha_2\delta$ subunits in cultured cells. Our data are inconsistent with some results of the recent report that alternative splicing determines properties of P- and Q-type Ca^{2+} channels. Bourinet *et al.* (18) reported that a non-inactivating current form, which was similar to a P-type one, was recorded when the $\alpha_1$2.1 subunit, containing a single valine insertion in repeat I–II linker, was co-expressed with $\alpha_2\delta$ and β_2 subunits. However, it is unlikely that native P-type current is encoded by this combination of subunits for the following reasons. First, our splice variants, MPI and MPII isolated from Purkinje cells, lack the single valine insertion. Second, the inactivation for MPI, MPII, or MPc channel became slower by co-expression of β_2 (Fig. 3*B*), however, it was still faster compared with the native P-type current (37).

Pharmacologically, P- and Q-type Ca^{2+} channels differ in the sensitivity to ω-Aga IVA. The P-type current is significantly blocked by ω-Aga IVA, with an IC_{50} value of 1–2 nM (42). In contrast, the Q-type current is less sensitive to ω-Aga IVA, with an IC_{50} of 89 nM (8). The sensitivity of MPI, MPII, and MPc channels were similar to that of Q-type channels. The sensitivity to ω-Aga IVA was shown to depend significantly on the type of cells where $\alpha_1$2.1 was expressed. For example, the IC_{50} value for rat rbA-1 is higher than 200 nM in *Xenopus* oocytes, whereas it is as low as 16.3 nM in HEK293 cells (18). Recently, it has been reported that splicing of $\alpha_1$2.1 also affects the toxin sensitivity: $\alpha_1$2.1 without arginine and proline (NP) insertion between segments S3 and S4 in repeat IV showed higher sensitivity (IC_{50} = 16.3 nM) than $\alpha_1$2.1 with the NP insertion (IC_{50} = 146 nM) (18). Because the sensitivity observed in HEK293 cells was still not as high as that in Purkinje cells, high sensitivity observed in Purkinje cells was expected to arise from the lack of NP insertion in $\alpha_1$2.1 together with the specific environment of Purkinje cells. Our results support this idea in the pharmacological respect, because MPI and MPII lacked the NP insertion.

In conclusion, our results suggest that MPI and MPII may distribute differently and play some specific roles in Purkinje cells. Further study is necessary to substantiate this point. MPI, MPII, and MPc cannot generate P-type currents in HEK293 cells, suggesting that alternative splice variants of $\alpha_1$2.1 subunit expressed in Purkinje cells alone are not sufficient to generate native P-type currents in heterologous expression system. Some specific environmental modifications such as post-translational processing or modulation by putative proteins associated with the channels may be necessary to generate the native P-type current.

Acknowledgments—We are grateful to Dr. S. Zong for the construction of expression plasmids for β_{2a} and β_3, Drs. S. Toru and M. Osanai for technical advice on the experiment and data analysis, Dr. Y. Kubo for critical advice on electrophysiological experiments, Drs. V. Flockerzi and F. Hofmann for providing the plasmids pBH19 and pBH23, Dr. E. Perez-Reyes for providing the plasmid βk213, and Dr. F. Chee for a sincere effort to improve the manuscript.

REFERENCES

1. Catterall, W. A. (1998) *Cell Calcium* **24,** 307–323
2. Dunlap, K., Luebke, J. I., and Turner, T. J. (1995) *Trends Neurosci.* **18,** 89–98
3. Ertel, E. A., Campbell, K. P., Harpold, M. M., Hofmann, F., Mori, Y., Perez-Reyes, E., Schwartz, A., Snutch, T. P., Tanabe, T., Birnbaumer, L., Tsien, R. W., and Catterall, W. A. (2000) *Neuron* **25,** 533–535
4. Takahashi, T., and Momiyama, A. (1993) *Nature* **366,** 156–158
5. Mintz, I. M., Adams, M. E., and Bean, B. P. (1992) *Neuron* **9,** 85–95
6. Wheeler, D. B., Randall, A., and Tsien, R. W. (1994) *Science* **264,** 107–111
7. Llinás, R., Sugimori, M., Lin, J.-W., and Cherksey, B. (1989) *Proc. Natl. Acad. Sci. U. S. A.* **86,** 1689–1693
8. Randall, A., and Tsien, R. W. (1995) *J. Neurosci.* **15,** 2995–3012
9. Wheeler, D. B., Randall, A., Sather, W. A., and Tsien, R. W. (1995) *Prog. Brain Res.* **105,** 65–78
10. Ophoff, R. A., Terwindt, G. M., Vergouwe, M. N., van Eijk, R., Oefner, P. J., Hoffman, S. M. G., Lamerdin, J. E., Mohrenweiser, H. W., Bulman, D. E., Ferrari, M., Haan, J., Lindhout, D., van Ommen, G.-J. B., Hofker, M. H., Ferrari, M. D., and Frants, R. R. (1996) *Cell* **87,** 543–552
11. Zhuchenko, O., Bailey, J., Bonnen, P., Ashizawa T., Stockton, D. W., Amos, C., Dobyns, W. B., Subramony, S. H., Zoghbi, H. Y., and Lee, C. C. (1997) *Nat. Genet.* **15,** 62–69
12. Ishikawa, K., Tanaka, H., Saito, M., Ohkoshi, N., Fujita, T., Yoshizawa, K., Ikeuchi, T., Watanabe, M., Hayashi, A., Takiyama, Y., Nishizawa, M., Nakano, I., Matubayashi, K., Miwa, M., Shoji, S., Kanazawa, I., Tsuji, S., and Mizusawa, H. (1997) *Am. J. Hum. Genet.* **61,** 336–346
13. Gomez, C. M., Thompson, R. M., Gammack, J. T., Perlman, S. L., Dobyns, W. B., Truwit, C. L., Zee, D. S., Clark H. B., and Anderson, J. H. (1997) *Ann. Neurol.* **42,** 933–950
14. Ishikawa, K., Watanabe, M., Yoshizawa, K., Fujita, T., Iwamoto, H., Yoshizawa, T., Harada, K., Nakamagoe, K., Komatsuzaki, Y., Satou, A., Doi, M., Ogata, T., Kanazawa, I., Shoji, S., and Mizusawa, H. (1999) *J. Neurol. Neurosurg. Psychiatry* **67,** 86–89
15. Matsuyama, Z., Wakamori, M., Mori, Y., Kawakami, H., Nakamura, S., and Imoto, K. (1999) *J. Neurosci.* **19,** 1–5
16. Toru, S., Murakoshi, T., Ishikawa, K., Saegusa, H., Fujigasaki, H., Uchihara, T., Nagayama, S., Osanai, M., Mizusawa, H., and Tanabe, T. (2000) *J. Biol. Chem.* **275,** 10893–10898
17. Restituito, S., Thompson, R. M., Eliet, J., Raike, R. S., Riedl, M., Charnet, P., and Gomez, C. M. (2000) *J. Neurosci.* **20,** 6394–6403
18. Bourinet, E., Soong, T. W., Sutton, K., Slaymaker, S., Mathews, E., Monteil, A., Zamponi, G. W., Nargeot, J., and Snutch, T. P. (1999) *Nat. Neurosci.* **2,** 407–415
19. Gillard, S. E., Volsen, S. G., Smith, W., Beattie, R. E., Bleakman, D., and Lodge, D. (1997) *Neuropharmacology* **36,** 405–409
20. Pinto, A., Gillard, S., Moss, F., Whyte, K., Brust P, Williams, M., Stauderman, K., Harpold, M., Lang, B., Newson-Davis, J., Bleakman, D., Lodge, D., and Boot, J. (1998) *Proc. Natl. Acad. Sci. U. S. A.* **95,** 8328–8333
21. Jun, K., Piedras-Rentería, E. S., Smith, S. M., Wheeler, D. B., Lee, S. B., Lee, T. G., Chin, H., Adams, M. E., Scheller, R. H., Tsien, R. W., and Shin H.-S. (1999) *Proc. Natl. Acad. Sci. U. S. A.* **96,** 15245–15250
22. Mori, Y., Friedrich, T., Kim, M.-S., Mikami, A., Nakai, J., Ruth, P., Bosse, E., Hofmann, F., Flockerzi, V., Furuichi, T., Mikoshiba, K., Imoto, K., Tanabe, T., and Numa, S. (1991) *Nature* **350,** 398–402
23. Starr, T. V., Prystay, W., and Snutch, T. P. (1991) *Proc. Natl. Acad. Sci. U. S. A.* **88,** 5621–5625
24. Krovetz, H. S., Helton, T. D., Crews, A. L., and Horne, W. A. (2000) *J. Neurosci.* **20,** 7564–7570
25. Hans, M., Urrutia, A., Deal, C., Brust, P. F., Stauderman, K., Ellis, S. B., Harpold, M. M., Johnson, E. C., and Williams, M. E. (1999) *Biophys. J.* **76,** 1384–1440
26. Sather, W. A., Tanabe, T., Zhang, J.-F., Mori, Y., Adams, M. E., and Tsien, R. W. (1993) *Neuron* **11,** 291–303
27. Lambolez, B., Audinat, E., Bochet, P., Crepel, F., and Rossier, J. (1992) *Neuron* **9,** 247–258
28. Miera, E. V.-S., Rudy, B., Sugimori, M., and Llinás, R. (1997) *Proc. Natl. Acad. Sci. U. S. A.* **94,** 7059–7064
29. Chomczynski, P., and Sacchi, N. (1987) *Anal. Biochem.* **167,** 156–159
30. Fletcher, C. F., Lutz, C. M., O'Sullivan, T. N., Shaughnessy, J. D., Jr., Hawkes, R., Frankel, W. N., Copeland, N. G., and Jenkins, N. A. (1996) *Cell* **87,** 607–617
31. Takahashi, E., Murata, Y., Oki, T., Miyamoto, N., Mori, Y., Takada, N., Wanifuchi, H., Wanifuchi, N., Yagami, K., Niidome, T., Tanaka, I., and Katayama, K. (1999) *Biochem. Biophys. Res. Commun.* **260,** 54–59
32. Zong, S., Zhou, J., and Tanabe, T. (1994) *Biochem. Biophys. Res. Commun.* **201,** 1117–1123
33. Hullin, R., Singer-Lahat, D., Freichel, M., Biel, M., Dascal, N., Hofmann, F., and Flockerzi, V. (1992) *EMBO J.* **11,** 885–890
34. Mishina, M., Kurosaki, T., Tobimatsu, T., Morimoto, Y., Noda, M., Yamamoto, T., Terao, M., Lindstrom, J., Takahashi, T., Kuno, M., and Numa, S. (1984) *Nature* **307,** 604–608
35. Castellano, A., Wei, X., Birnbaumer, L., and Perez-Reyes, E. (1993) *J. Biol. Chem.* **268,** 12359–12366
36. Ligon, B., Boyd, A. E., III, and Dunlap, K. (1998) *J. Biol. Chem.* **273,** 13905–13911
37. Regan, L. J. (1991) *J. Neurosci.* **11,** 2259–2269
38. Moreno, H., Rudy, B., and Llinás, R. (1997) *Proc. Natl. Acad. Sci. U. S. A.* **94,** 14042–14047
39. Sommer, B., Köhler, M., Sprengel, R., and Seeburg, P. H. (1991) *Cell* **67,** 11–19
40. Maximov, A., Südhof, T. C., and Bezprozvanny, I. (1999) *J. Biol. Chem.* **274,** 24453–24456
41. Stea, A., Tomlinson, J., Soong, T. W., Bourinet, E., Dubel, S. J., Vincent, S. R., and Snutch, T. P. (1994) *Proc. Natl. Acad. Sci. U. S. A.* **91,** 10576–10580
42. Mintz, I. M., Venema, V. J., Swiderek, K. M., Lee, T. D., Bean, B. P., and Adams, M. E. (1992) *Nature* **355,** 827–829

J Neurol (2002) 249 : 633–635

Shinji Ohara
Teruaki Iwahashi
Takashi Oide
Ryoichi Hayashi
Takashi Nakajima
Kinya Ishikawa
Hidehiro Mizusawa

Spinocerebellar ataxia type 6 with motor neuron loss: A follow-up autopsy report

Received: 12 May 2001
Received in revised form:
26 November 2001
Accepted: 4 December 2001

Sirs: We have reported previously a Japanese patient with SCA6 gene mutation who had developed a lower motor neuron syndrome together with cerebellar ataxia [1]. We then speculated that this unusual clinical constellation could be either a chance co-occurrence of SCA6 and motor neuron disease or could be ascribed to a mutated SCA6 gene, identical to the α1A-voltage-dependent-calcium channel subunit gene (*CACNL1A4*), possibly affecting metabolic steps common to Purkinje cells and motor neurons. The following is the follow-up autopsy report for this patient, which unequivocally reveals co-existence of two distinct pathologies of SCA6 and ALS.

Briefly, the patient presented with dysarthria, ataxic gait, and left foot drop at age 58. She also had nystagmus and complained of occasional diplopia and vertigo. Her family history was positive for ataxic gait in her father. No other family members developed signs of motor neuron disorder with or without ataxia. Within the next 3 years, she developed progressive muscle weakness and atrophy and was placed on a respirator at age 61. She died of acute circulatory collapse of unknown etiology at age 64. Her mental status was completely normal up until only a few hours before her unexpected death.

The autopsy was performed 1 hour after death. The brain was small and weighed 920 g. Macroscopically, the cerebellum, especially in the upper part of the vermis and the pyramis in the medulla oblongata, was atrophic (Fig. A). Histologically, the loss of Purkinje cells was most marked in the vermis and the upper portion of the superior semilunar lobules associated with thinning of the molecular layer and loss of granular cells. Immunocytochemistry for the α1A calcium channel protein revealed cytoplasmic aggregations in Purkinje cells. No ubiquitin-immunoreactive nuclear inclusions were found in the cerebellum. The dentate nucleus was well-preserved. The substantia nigra showed mild neuronal loss, with the presence of extracellular melanin pigment. The pons was histologically normal. In the medulla oblongata, the hypoglossal nucleus showed severe neuronal loss. The rostral and dorsal parts of the principal inferior olivary nuclei revealed obvious neuronal loss and gliosis, but not comparable to the severe degree seen in the upper portion of the cerebellar vermis. The pyramis was atrophic and was pale on myelin stain. In the cerebrum, the number of large pyramidal neurons in the motor cortex was decreased, otherwise the cerebral cortex, white matter, basal ganglia, and thalamus were unremarkable. In the spinal cord, the corticospinal and spinocerebellar tracts revealed myelin pallor (Fig. B). There was a severe loss of neurons in the anterior horn. In the remaining neurons, Bunina bodies and ubiquitin-immunoreactive intracytoplasmic skein-like inclusions were occasionally present (Fig. C). Immunohistochemisty for the α1A channel protein failed to reveal any affregates in the remaining anterior horn cells. The Clarke nuclei showed a decreased number of neurons and the Onufrowitz nuclei was intact. Anterior spinal roots in the cervical, lumbar spinal segments showed a marked loss of myelinated fibers (Fig. D). There was no loss in neurons in the dorsal root ganglion and autonomic ganglion.

In the present case, the autopsy revealed clinically unsuspected upper motor neuron degeneration in addition to lower motor neuron loss in the spinal cord and lower brainstem motor nuclei. The motor neuron loss was associated with the appearance of intracytoplasmic inclusions including Bunina bodies and ubiquitin-immunoreactive skein-like inclusions which are the histological hallmark of ALS [2]. The apperance of these intracytoplasmic inclusions has not been reported in SCA6, although it is worthy of note that slkein-like ubiquitin-positive deposits in the anterior horn cells and brain stem motor neurons have been described in a patient with SCA3 [3]. Indeed, upper motor neurons signs are regularly seen in SCA3 with onset before the age of 40 years and the axonal neuropathy is present in the age-related manner in this disease [4, 5]. It should also be mentioned that in the previous autopsy studies of SCA6, one patient revealed axonal degeneration in the corticospinal tract below the level of the medulla [6]. On the other hand, features of pure cerebellar degeneration were also evident in the present case. The dentate and pontine nuclei were well preserved, and the loss of Purkinje cells was predominantly in the upper vermis and the upper cerebellar hemisphere. These features of cerebellar lesions were consistent with those of the previous autopsy cases of